Supplementary Material for:

Iwona Stelniec-Klotz, Stefan Legewie, Oleg Tchernitsa, Franziska Witzel, Bertram Klinger, Christine Sers, Hanspeter Herzel, Nils Blüthgen and Reinhold Schäfer:

Reverse-engineering a hierarchical regulatory network downstream of oncogenic KRAS

Content (9 Figures, 3 Tables, 1 Text, 1 List of References)

Supplementary Figures

Supplementary Tables

Supplementary Texts

Supplementary References

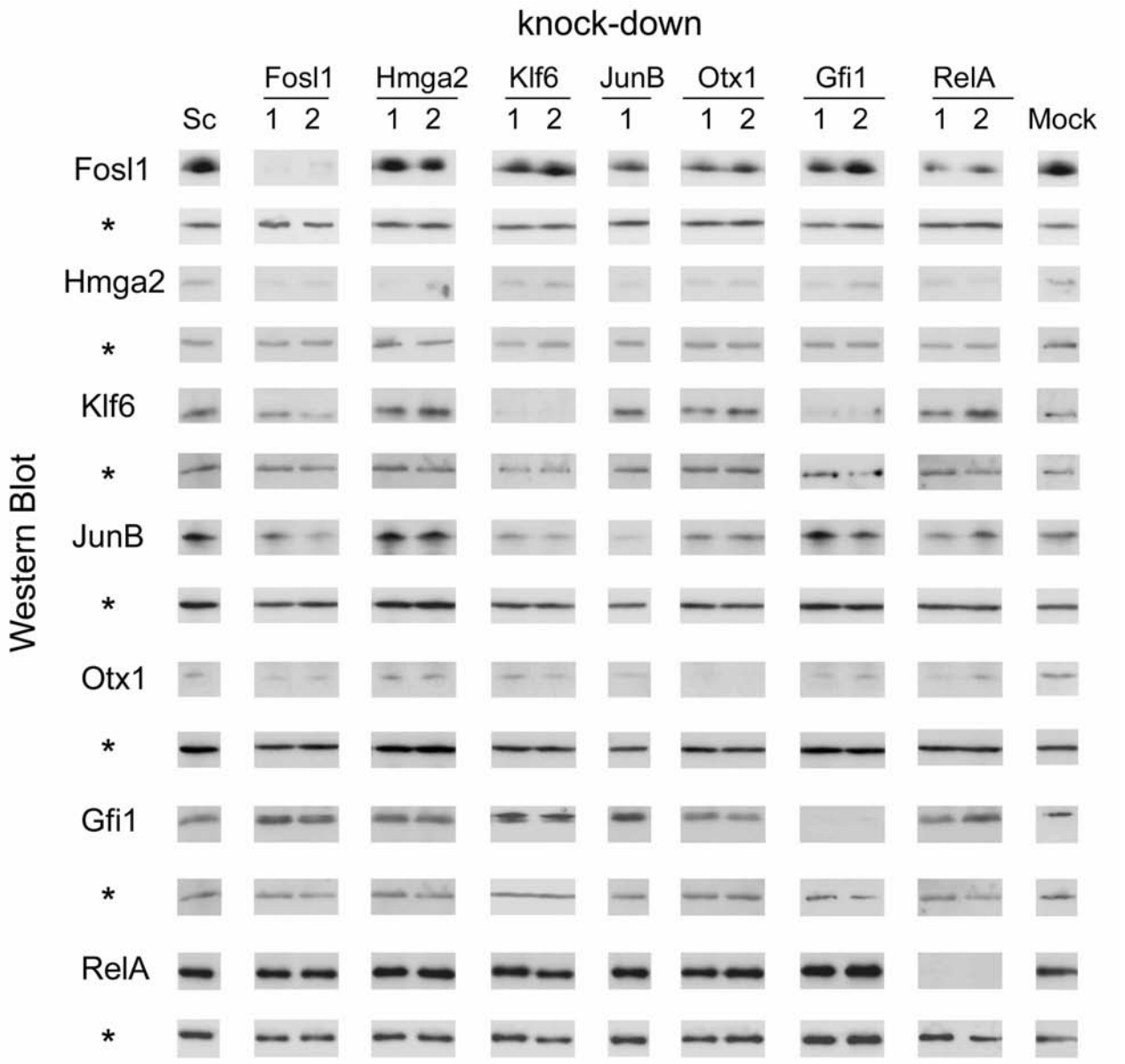

Supplementary Fig. 1 *Nuclear protein levels of Fosl1, Hmga2, Klf6, JunB, Otx1, Gfi1, RelA after silencing in KRAS-transformed RAS-ROSE cells.*

Western Blot analysis of nuclear protein levels of Fosl1, Hmga2, Klf6, JunB, Otx1, Gfi1 and RelA in RAS-ROSE cells 48 h after transfections with scrambled siRNAduplex (Sc), transfection reagents only (Mock) and two independent transcription factor specific siRNAs (1, 2). ß-tubulin control (*). One example of two biological replica is shown.

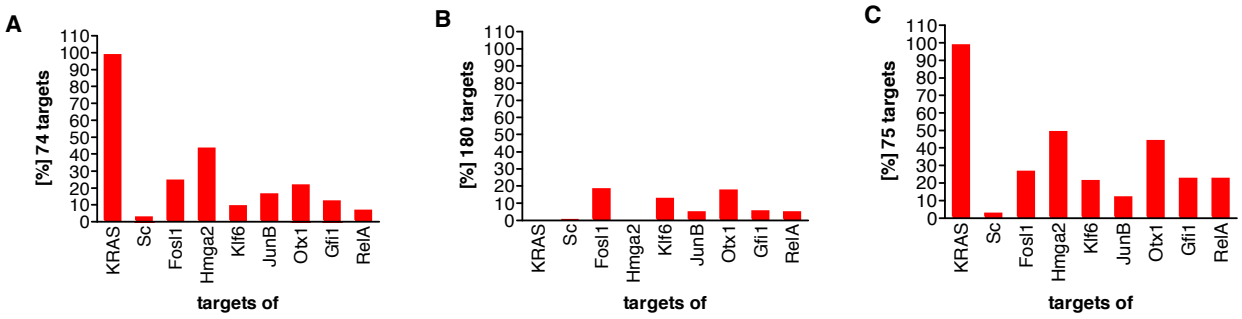

Supplementary Fig. 2 *Impact of transcription factor knock-down on the KRAS pathway-mediated mRNA expression profile.*

RNA expression profiles of KRAS transformed RAS-ROSE cells relative to non-transformed ROSE cells and of RAS-ROSE cells treated with scrambled siRNA-duplex (Sc) relative to RAS-ROSE cells treated with two independent siRNAs against Fosl1, Hmga2, Klf6, JunB, Otx1, Gfi1, RelA prepared in microarray analysis. Percentage of down regulated (A), none regulated (B) and up regulated (C) targets in RAS-ROSE cells after treatment with scrambled siRNA-duplex (Sc), transfection reagents only (Mock) and two independent transcription factor specific siRNAs (1, 2) in comparison to RAS-dependent regulated target genes (RAS-ROSE cells versus ROSE cells).

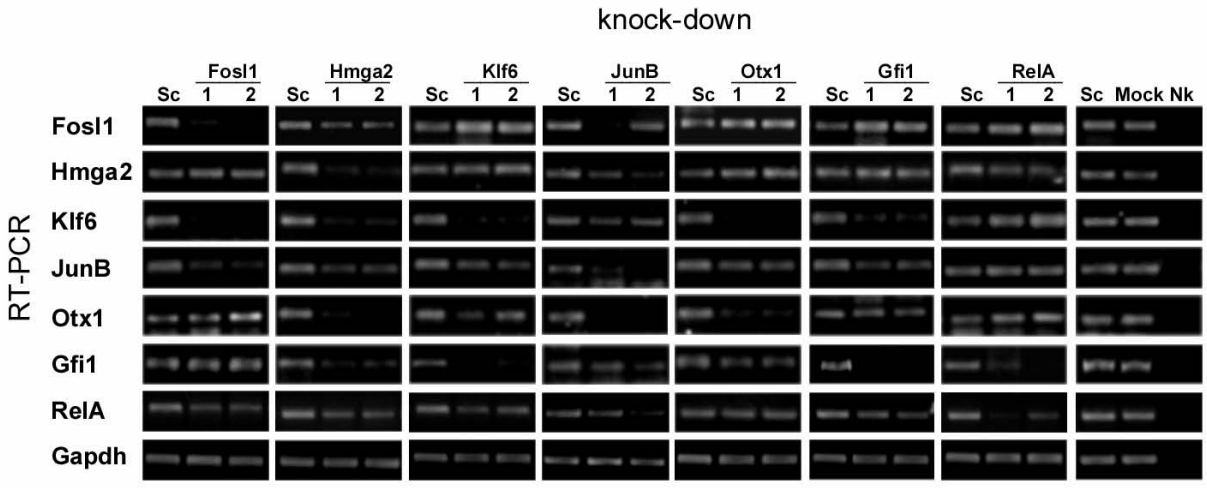

Supplementary Fig. 3 *RNA Expression of Fosl1, Hmga2, Klf6, JunB, Otx1, Gfi1, RelA after silencing in KRAS-transformed RAS-ROSE cells.*

RT-PCR analysis of RNA expression of Fosl1, Hmga2, Klf6, JunB, Otx1, Gfi1 and RelA in RAS-ROSE cells 48 h after transfections with scrambled siRNA-duplex (Sc), transfection reagents only (Mock) and two independent transcription factor specific siRNAs (1, 2). Control: Gapdh, Nk: negative control, H_2O. One example of two independent experiments is shown.

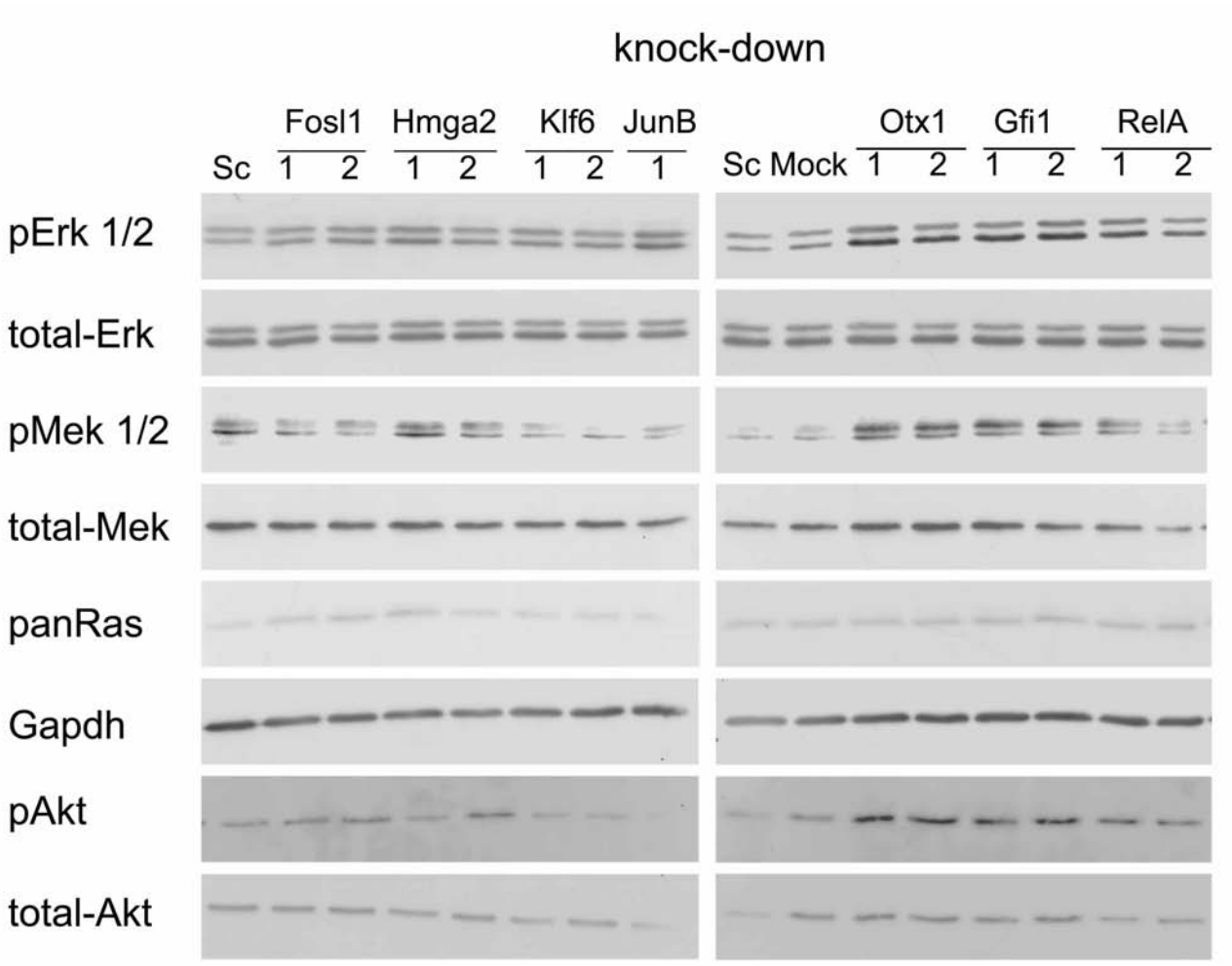

Supplementary Fig. 4 *Effects of Fosl1, Hmga2, Klf6, JunB, Otx1, Gfi1, RelA knock-down in RAS-ROSE cells on the activity of cytoplasmatic signaling downstream of RAS.*

Western Blot analysis of phosphorylation of Mek, Erk and Akt 48 h after transfections of Fosl1, Hmga2, Klf6, JunB, Otx1,Gfi1 and RelA in RAS-ROSE cells with two independent transcription factor specific siRNAs (1, 2). Scrambled siRNAduplex (Sc), transfection reagents only (Mock). Loading control for pMek, pErk, pAkt (total Mek, Erk, Akt), control for panRAS (Gapdh). One example of two biological replica is shown.

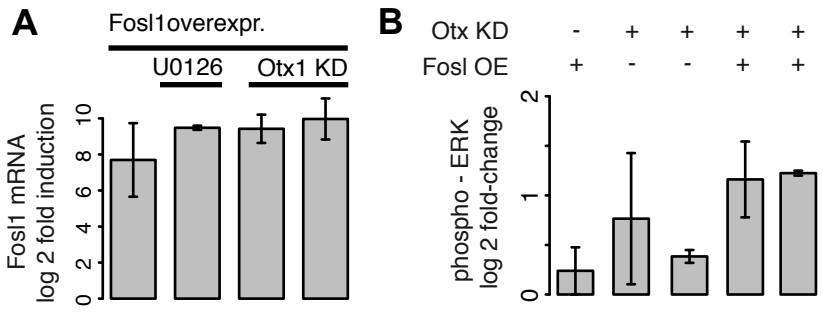

Supplementary Fig. 5 *Effect of Fosl1 overepxression and Otx1 knockdown on Fosl1 mRNA and phospho-Erk.*

mRNA levels of ectopically expressed Fosl1 are not influenced by Mek inhibition with U0126, or knockdown of Otx1. Phoshpho-Erk levels tend to rise upon Fosl overexpression and Otx knockdown,

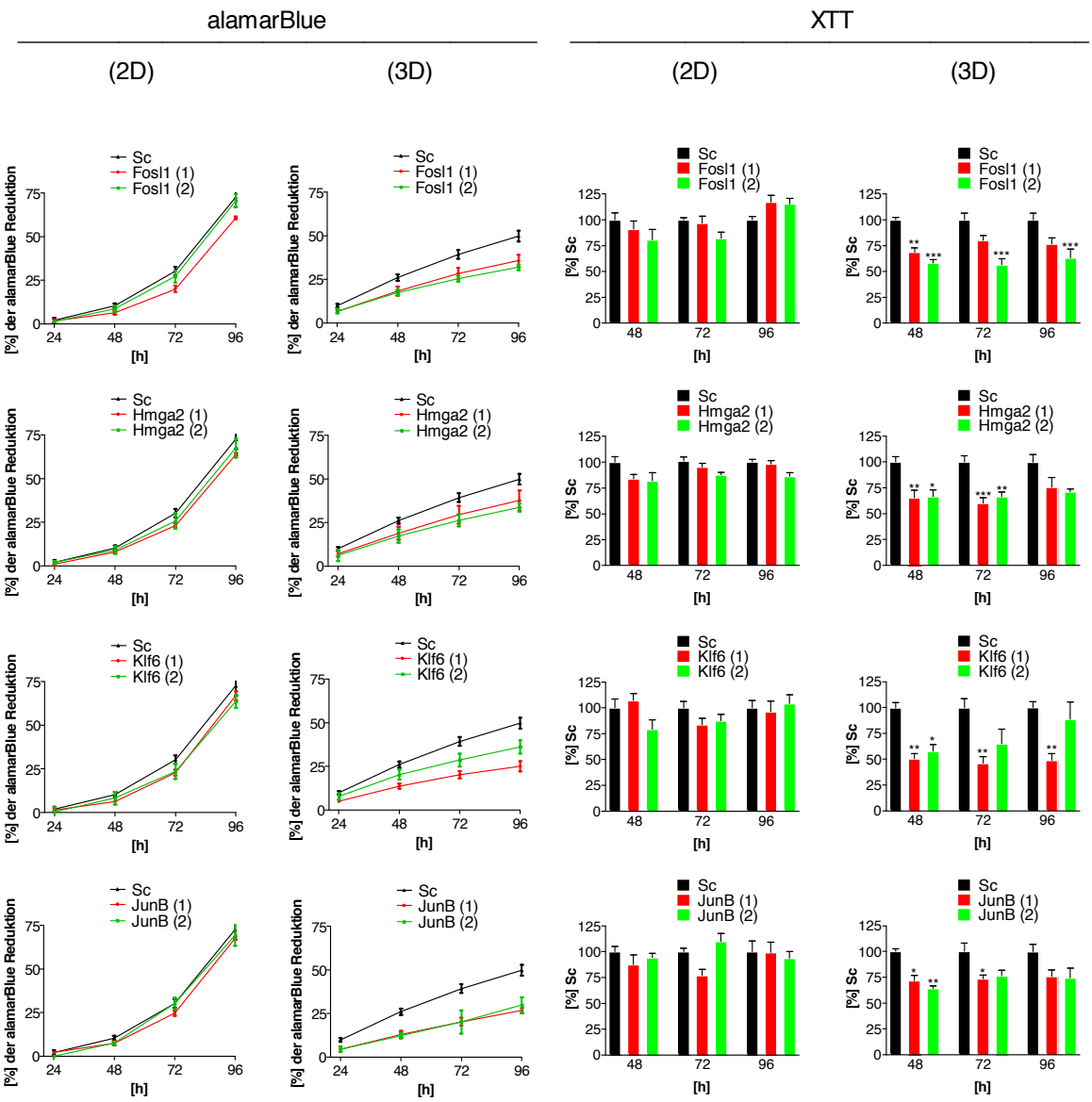

Supplementary Fig. 6 *Effects on growth characteristics of RAS-ROSE cells after silencing of Fosl1, Hmga2, Klf6 and JunB.*

Results from analysis of anchorage-dependent (2D) and anchorage-independent (3D) growth of RAS-ROSE cells 48-96 h after treatment with scrambled siRNA-duplex (Sc) and two independent transcription factor specific siRNAs (1, 2) determined by calorimetric XTT and alamarBlue assays. The values from XTT test correspond in percent to Sc. Results of one representative amalarBlue test and of 2-3 independently biological XTT tests were illustrated. The continuously measurement of alamarBlue test is illustrated as line graph. P 0,05; ** P 0,01; *** P 0,001.

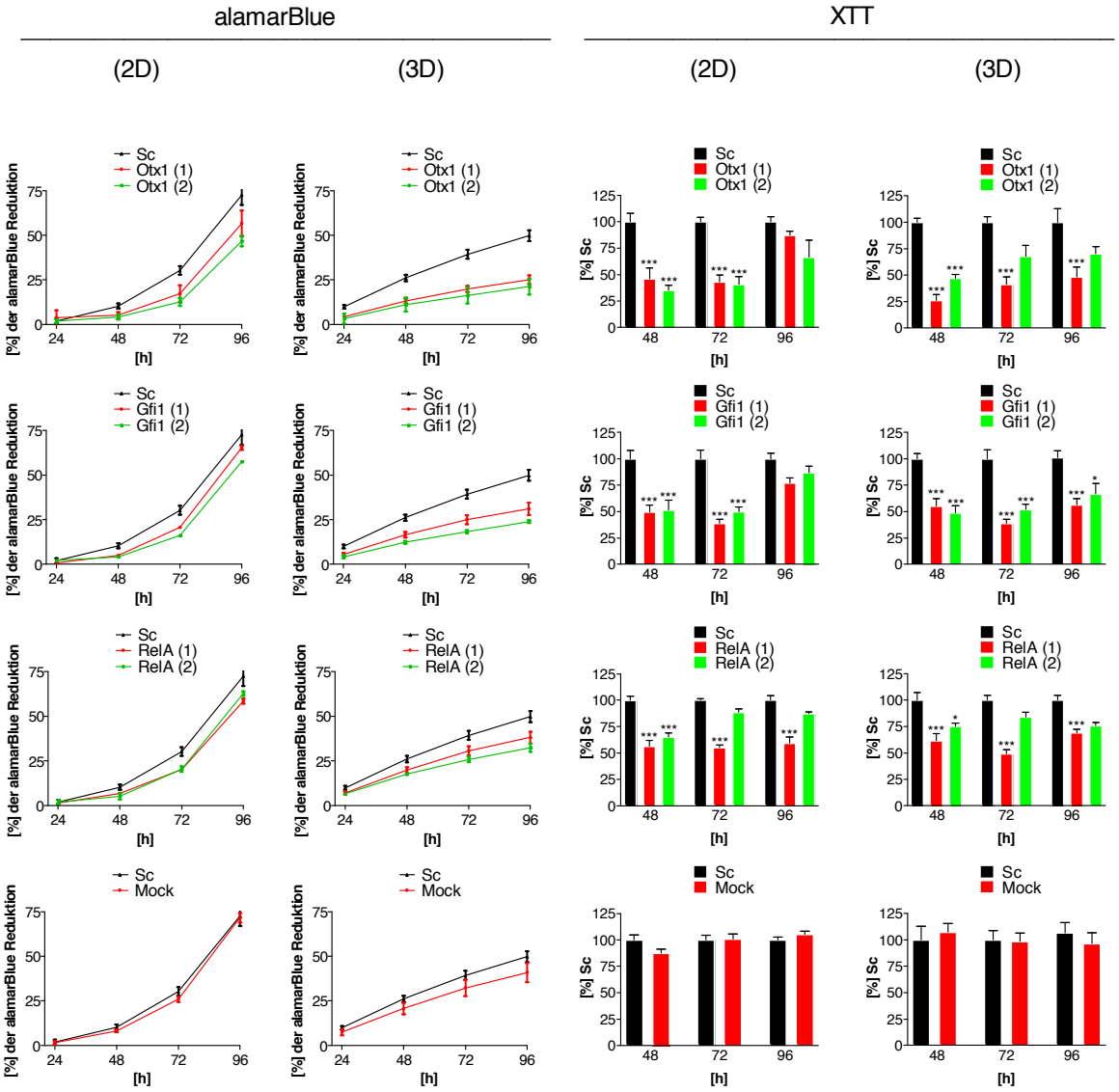

Supplementary Fig. 7 *Effects on growth characteristics of RAS-ROSE cells after silencing of Otx, Gfi1 and RelA.*

Results from analysis of anchorage-dependent (2D) and anchorage-independent (3D) growth of RAS-ROSE cells 48-96 h after last treatment with scrambled siRNA-duplex (Sc), transfection reagents only (Mock), two independent transcription factor specific siRNAs (1, 2) determined by calorimetric XTT and alamarBlue assays. Results of one representative amalarBlue test and of 2-3 independently biological XTT tests were pictured. The continuously measurement of alamarBlue test is illustrated as line graph. P 0,05; ** P 0,01; *** P 0,001.

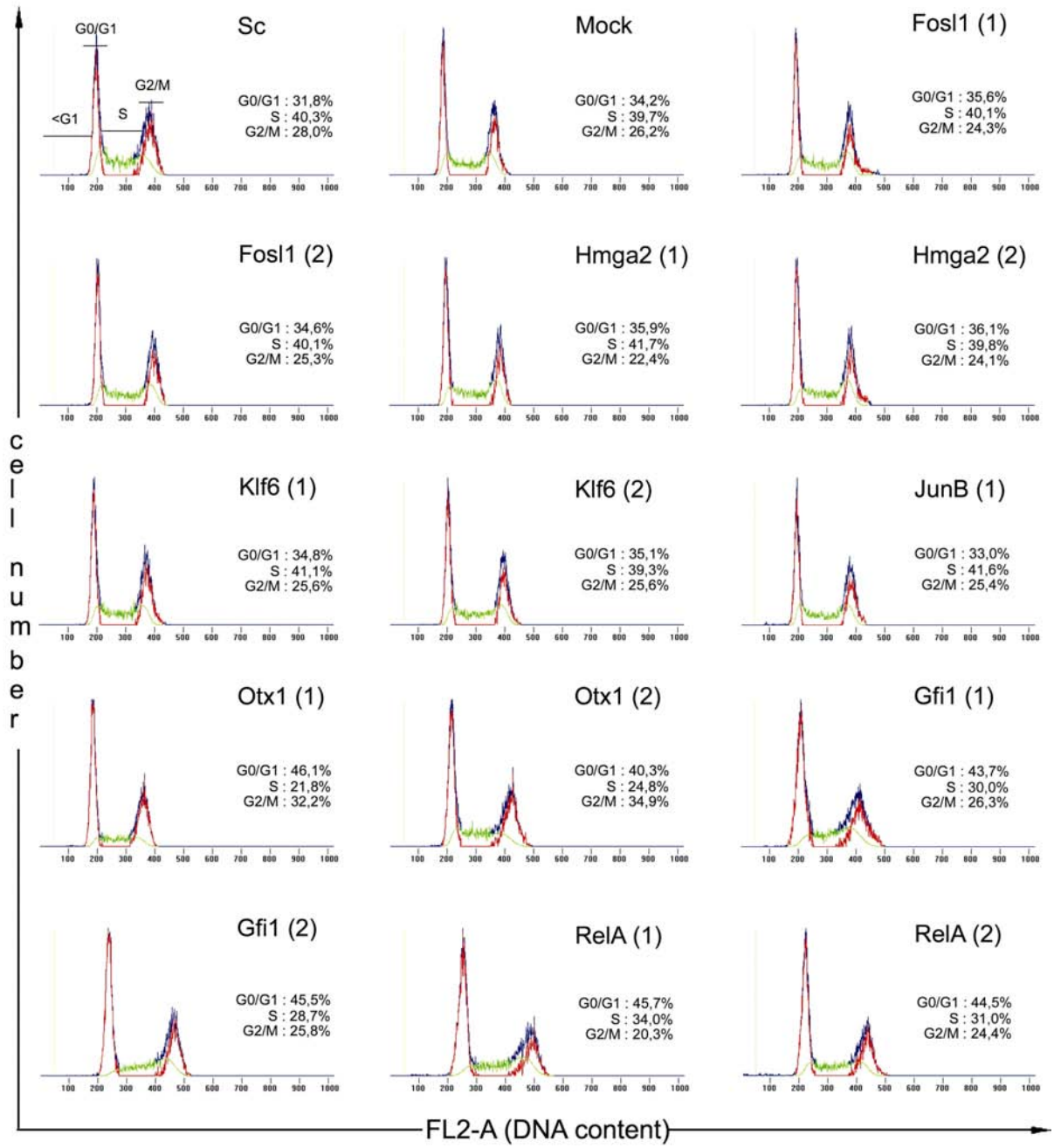

Supplementary Fig. 8 *Effects on distribution of cell cycle phases in KRAS-transformed RAS-ROSE cells after silencing of Fosl1, Hmga2, Klf6, JunB, Otx1, Gfi1, RelA.*

Results from cell cycle analysis of RAS-ROSE cells 48 h after treatment with scrambled siRNA-duplex (Sc), transfection reagents only (Mock) and two independent transcription factor specific siRNAs (1, 2). Distribution of cells to cell cycle phases G0/G1, S and G2/M was determined by FACS analysis after DNA staining of cells with propidium iodide.

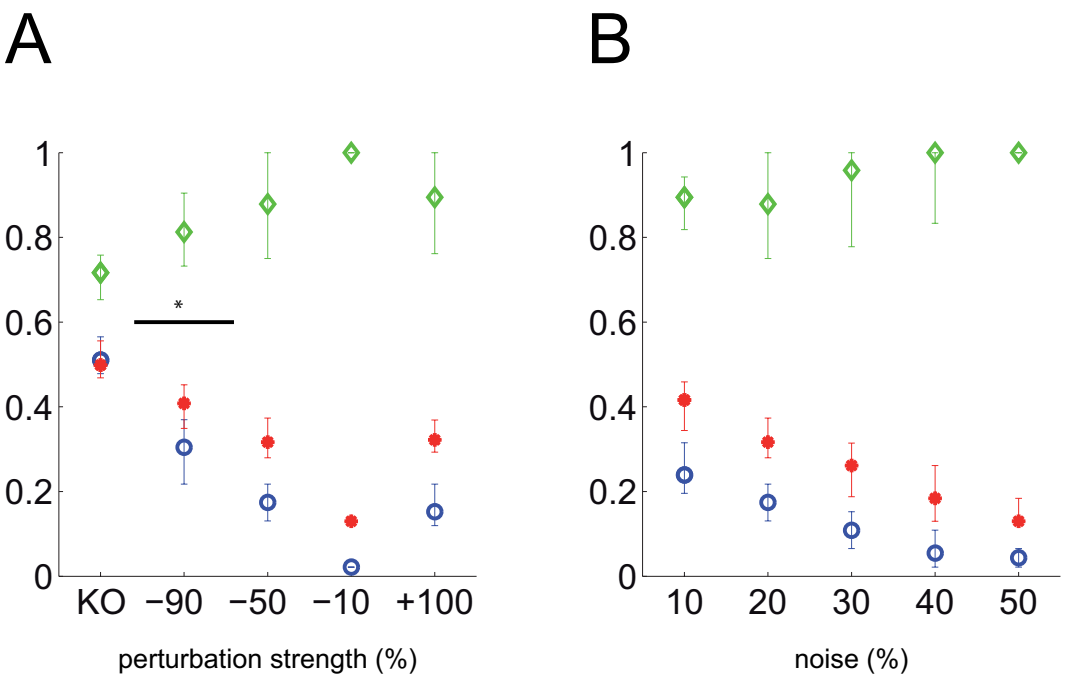

*experimental KD efficiency range

Supplementary Fig. 9: *Effect of perturbation strength and noise on algorithm performance.*

Precision (green diamonds), sensitivity (blue open circles) and Matthew's correlation coefficient (red filled circles) for simulated networks of 10 nodes. One hundred randomly generated networks were simulated, each having a connectivity of 40% of possible interactions between genes (the kinetic parameters were sampled from log-normal distributions). Each data point represents the median of simulations with 1st and 3rd quartile indicated as whiskers. (A) Variation of perturbation strength effects predictability. Median precision was typically above 80%, and slightly lower for very strong knockouts. Note that only non-trivial predictions were counted (i.e. translation was not counted), and that the algorithm typically did not find weak links. Noise level was kept at 20%. Conditions for the experimental data presented are indicated with a black bar. (B) Effect of noise level on algorithm performance. Median precision was generally above 80%, and precision dropped slightly for low noise levels. The sensitivity decreases strongly with increased noise level, whereas the precision even increases slightly. Initial perturbation was set to -50%. See supplementary text for details.

Supplementary Table S1: *Rules for finding transcription factor-related patterns in genome-wide expression data (related to Fig. 3B and C).*
A probe set was defined as 'matching the transcription factor pattern' if the above constraints are fulfilled over *all* knockdown conditions. Different constraints were used for transcription factor mRNA and protein patterns, since fold changes at the protein level are typically much higher: Constraints 1-5 were used to relate transcription factor protein patterns, while 6-10 apply for mRNA patterns. Fixed constraints for the probe sets were used for large or absent changes in transcription factor levels (#1, #3, #5, #6, #8, #10). Flexible constraints depending on the fold-change in the transcription factor levels (X) were employed for intermediate responses (#2, #4, #7 and #9). A probe set needs to match the criteria in column 3 or 4 for all seven knockdown conditions to appear in Fig. 3B and C.

#	TF pattern	Transcription factor (log-fold-change)	Constraints for log-fold changes in probe sets (correlated)	Constraints for log-fold changes in probe sets (anti-correlated)
1	protein	> 0.9	> 0.5	< -0.5
2		0.2 to 0.9	> X – 1 $\wedge$ < X + 1	> -X - 1 $\wedge$ < -X + 1
3		-0.2 to 0.2	< 0.7 $\wedge$ > -0.7	<0.7 $\wedge$ >-0.7
4		-0.9 to -0.2	> X – 1 $\wedge$ < X + 1	> -X – 1 $\wedge$ < -X + 1
5		< -0.9	< -0.5	> 0.5
6	mRNA	>0.5	Same as protein	Same as protein
7		0.2to 0.5		
8		-0.2 to 0.2		
9		-0.5 to -0.2		
10		<-0.5		

Supplementary Table S2: *Known interaction (related to Fig. 4)*

Section	Interaction	Reference	Comment
5	Gfi1 mRNA -> Gfi1 protein	-	mRNA translation
5	Otx1 mRNA -> Otx1 protein	-	mRNA translation
5	RelA mRNA -> RelA protein	-	mRNA translation
5	FosL1 mRNA -> FosL1 protein	-	mRNA translation
5	KLF6 mRNA -> KLF6 protein	-	mRNA translation
5	JunB mRNA -> JunB protein	-	mRNA translation
5	HMGA2 mRNA -> HMGA2 protein	-	mRNA translation
7	Ras -> pAkt	-	signalling
7	Ras -> pErk	-	signalling
1	pErk -> HMGA2 mRNA	(Lee & Dutta, 2007; Merchant et al, 1999; Paroo et al, 2009; Rustighi et al, 1999)	via Erk-mediated activation of Sp1/NF-1 transcription factors; Erk inhibits let-7 miRNA processing
1	pErk -> Fosl1 mRNA	(Adiseshaiah et al, 2008; Adiseshaiah et al, 2005; Vial & Marshall, 2003)	via TCF proteins
1	pErk -> Gfi-1 mRNA	(Shinnakasu et al, 2008)	Gfi-1 mRNA is induced by Erk
1	pErk -> Otx-1 mRNA	(Bertrand et al, 2003)	Ascidian otx (most closely related to Otx-2) is induced by Erk-dependent Ets factors
4	Akt -> RelA protein	(Madrid et al, 2000)	Akt phosphorylates and activates RelA
4	pErk -| HMGA2 protein	(Di Agostino et al, 2004)	Erk activates Nek2 kinase which deactivates HMGA2 binding to DNA
9	RelA protein -| pErk	(Ahmed et al, 2006)	
9	Fosl1 protein -| pAkt	(Ramos-Nino et al, 2008)	Overexpression of Fosl1 decreases Akt activation
9	KLF6 protein -| pErk	(Amit et al, 2007; Liu et al)	KLF6 binds Src and thereby inhibits Erk activation; KLF6 knockdown increases Erk-induced transcription
3	Fosl1 protein -> JunB mRNA	(Casalino et al, 2007)	Fra1 overexpression decreases and Fra1 knockdown increases JunB expression
3	RelA protein -> HMGA2 mRNA	(Iliopoulos et al, 2009)	NF-kB reduces let-7 leves, and let-7 is an inhibitor of HMGA2 expression
3	RelA protein -> Otx1 mRNA	(Lake et al, 2001)	NF-kB induces Otx-2 expression in Xenopus
3	KLF6 protein -> Fra-1 mRNA	(Huntley et al, 2004; Narla et al, 2003)	KLF6 modulates TGFbeta signalling, a known modulator of Fra-1 expression

Supplementary Table S3: *Quantification of the network.*
For each edge in the network , the response coefficient is provided. The increase in Chi2-Value when a model without that edge was fitted to the data was used to calculate a p-value (likelihood ration test).

Source	Target	Response coefficient	Increase in Chi2	p-value (log 10)
Fosl1 RNA	Fosl1 Prot	2.18	205.53	-45.89
Otx1 RNA	Otx1 Prot	1.36	171.05	-38.36
JunB RNA	JunB Prot	1.83	131.26	-29.66
Klf6 RNA	Klf6 Prot	1.59	124.23	-28.13
Hmga2 RNA	Hmga2 Prot	2.29	116.66	-26.47
Fosl1 Prot	JunB RNA	0.42	114.34	-25.96
Gfi1 RNA	Gfi1 Prot	1.88	105.12	-23.94
RAS	pERK	1.56	103.08	-23.49
Rela RNA	RelA Prot	3.76	75.53	-17.44
pERK	Hmga2 RNA	0.99	50.16	-11.85
pERK	Hmga2 Prot	-2.20	44.26	-10.54
pAKT	RelA Prot	0.47	32.47	-7.92
Klf6 Prot	Fosl1 RNA	0.24	31.71	-7.75
Otx1 Prot	Fosl1 RNA	0.29	31.04	-7.60
RelA Prot	Otx1 RNA	0.37	24.25	-6.07
Klf6 Prot	pERK	-0.60	23.96	-6.01
Gfi1 Prot	Otx1 RNA	0.34	23.21	-5.84
pERK	Fosl1 Prot	-1.51	22.96	-5.78
pERK	Fosl1 RNA	0.68	22.94	-5.78
JunB Prot	Klf6 RNA	0.40	22.14	-5.60
Otx1 Prot	pAKT	-0.83	21.93	-5.55
Rela Prot	Hmga2 RNA	0.30	18.76	-4.83
pERK	Gfi1 RNA	0.30	17.50	-4.54
JunB Prot	pAKT	3.22	16.92	-4.41
Gfi1 Prot	Klf6 RNA	0.33	16.48	-4.31
Otx1 Prot	Gfi1 RNA	0.26	14.58	-3.87

Supplementary Text: Generation of artificial data sets

To assess the prediction quality of the method, we used simulated data sets for randomly generated networks that consisted of 10 genes which regulate each other by transcriptional induction or repression. The network was simulated using an ODE-model following the approach described in (Mendes et al, 2003). Briefly, evolution of the mRNA levels were calculated using the following differential equation:

$$\frac{d[RNA_i]}{dt} = V_{max} \prod_j (1 + \frac{[P_j]^{n_j}}{[P_j]^{n_j} + {K_j}^{n_j}}) \prod_k (\frac{{K_k}^{n_k}}{[P_k]^{n_k} + {K_k}^{n_k}}) - d_{rna,i}[RNA_i]$$

and protein levels (P_i) were modelled using the differential equation:

$$\frac{d[P_i]}{dt} = k_i[RNA_i] - d_{P,i}[P_i]$$

Network structures were generated by randomly setting V_{max} = 0 for 60% of the mRNAs in the network (i.e., the networks had a connectivity of 40% of possible interactions).

The remaining kinetic parameters were sampled from log-normal distributions: The degradation rates (d's), and Vmax's where drawn from a log normal distribution (ln *N*(0,1)). The K's were also drawn from ln *N*(0,1), but divided by two so that they are on average half of the mean of Vmax. Hill coefficients (n's) where drawn from a log normal distribution ln *N*(0,0.27) and multiplied by 2.5.

We simulated perturbation experiments by first determining the unperturbed steady state of the system and, second, by determining the new steady states after changing each mRNA production rate. After calculating the state of the network near the steady state, noise is applied to the unperturbed as well as to the perturbed network. From these values, we calculated the matrix R as in the main manuscript. The Gaussian noise added was composed of multiplicative noise and additive noise. Whereas multiplicative noise depending only on the value it is added to, the additive noise was scaled to the average signal. Noise was assumed to consist of ¼ additive noise and ¾ multiplicative noise. For example, at 20% noise level, additive noise had a magnitude of 5% of the average signal, and 15% multiplicative noise (Supplementary Fig. S9 A). For investigating the effect of variations of the total noise level, we changed the total noise level, but left the additive to multiplicative ratio the same (1:3) (Supplementary Fig. S9 B). All simulations where implemented and carried out in MATLAB.

Supplementary References

Adiseshaiah P, Li J, Vaz M, Kalvakolanu DV, Reddy SP (2008) ERK signaling regulates tumor promoter induced c-Jun recruitment at the Fra-1 promoter. Biochem Biophys Res Commun 371: 304-308

Adiseshaiah P, Peddakama S, Zhang Q, Kalvakolanu DV, Reddy SP (2005) Mitogen regulated induction of FRA-1 proto-oncogene is controlled by the transcription factors binding to both serum and TPA response elements. Oncogene 24: 4193-4205

Ahmed KM, Dong S, Fan M, Li JJ (2006) Nuclear factor-kappaB p65 inhibits mitogen-activated protein kinase signaling pathway in radioresistant breast cancer cells. Mol Cancer Res 4: 945-955

Amit I, Citri A, Shay T, Lu Y, Katz M, Zhang F, Tarcic G, Siwak D, Lahad J, Jacob-Hirsch J, Amariglio N, Vaisman N, Segal E, Rechavi G, Alon U, Mills GB, Domany E, Yarden Y (2007) A module of negative feedback regulators defines growth factor signaling. Nature genetics 39: 503-512

Bertrand V, Hudson C, Caillol D, Popovici C, Lemaire P (2003) Neural tissue in ascidian embryos is induced by FGF9/16/20, acting via a combination of maternal GATA and Ets transcription factors. Cell 115: 615-627

Casalino L, Bakiri L, Talotta F, Weitzman JB, Fusco A, Yaniv M, Verde P (2007) Fra-1 promotes growth and survival in RAS-transformed thyroid cells by controlling cyclin A transcription. EMBO J 26: 1878-1890

Di Agostino S, Fedele M, Chieffi P, Fusco A, Rossi P, Geremia R, Sette C (2004) Phosphorylation of high-mobility group protein A2 by Nek2 kinase during the first meiotic division in mouse spermatocytes. Mol Biol Cell 15: 1224-1232

Huntley SP, Davies M, Matthews JB, Thomas G, Marshall J, Robinson CM, Eveson JW, Paterson IC, Prime SS (2004) Attenuated type II TGF-beta receptor signalling in human malignant oral keratinocytes induces a less differentiated and more aggressive phenotype that is associated with metastatic dissemination. Int J Cancer 110: 170-176

Iliopoulos D, Hirsch HA, Struhl K (2009) An epigenetic switch involving NF-kappaB, Lin28, Let-7 MicroRNA, and IL6 links inflammation to cell transformation. Cell 139: 693-706

Lake BB, Ford R, Kao KR (2001) Xrel3 is required for head development in Xenopus laevis. Development 128: 263-273

Lee YS, Dutta A (2007) The tumor suppressor microRNA let-7 represses the HMGA2 oncogene. Genes Dev 21: 1025-1030

Liu J, Du T, Yuan Y, He Y, Tan Z, Liu Z KLF6 inhibits estrogen receptor-mediated cell growth in breast cancer via a c-Src-mediated pathway. Mol Cell Biochem 335: 29-35

Madrid LV, Wang CY, Guttridge DC, Schottelius AJ, Baldwin AS, Jr., Mayo MW (2000) Akt suppresses apoptosis by stimulating the transactivation potential of the RelA/p65 subunit of NF-kappaB. Mol Cell Biol 20: 1626-1638

Mendes P, Sha W, Ye K (2003) Artificial gene networks for objective comparison of analysis algorithms. Bioinformatics, 19: ii122-ii129.

Merchant JL, Du M, Todisco A (1999) Sp1 phosphorylation by Erk 2 stimulates DNA binding. Biochem Biophys Res Commun 254: 454-461

Narla G, Friedman SL, Martignetti JA (2003) Kruppel cripples prostate cancer: KLF6 progress and prospects. Am J Pathol 162: 1047-1052

Paroo Z, Ye X, Chen S, Liu Q (2009) Phosphorylation of the human microRNA-generating complex mediates MAPK/Erk signaling. Cell 139: 112-122

Ramos-Nino ME, Blumen SR, Sabo-Attwood T, Pass H, Carbone M, Testa JR, Altomare DA, Mossman BT (2008) HGF mediates cell proliferation of human mesothelioma cells through a PI3K/MEK5/Fra-1 pathway. Am J Respir Cell Mol Biol 38: 209-217

Rustighi A, Mantovani F, Fusco A, Giancotti V, Manfioletti G (1999) Sp1 and CTF/NF-1 transcription factors are involved in the basal expression of the Hmgi-c proximal promoter. Biochem Biophys Res Commun 265: 439-447

Shinnakasu R, Yamashita M, Kuwahara M, Hosokawa H, Hasegawa A, Motohashi S, Nakayama T (2008) Gfi1-mediated stabilization of GATA3 protein is required for Th2 cell differentiation. J Biol Chem 283: 28216-28225

Vial E, Marshall CJ (2003) Elevated ERK-MAP kinase activity protects the FOS family member FRA-1 against proteasomal degradation in colon carcinoma cells. J Cell Sci 116: 4957-4963